



ELSEVIER

Contents lists available at [ScienceDirect](#)

HardwareX

journal homepage: www.elsevier.com/locate/ohx

Professor: A motorized field-based phenotyping cart

Alison L. Thompson^{a,*}, Alex Conrad^a, Matthew M. Conley^a, Henry Shrock^{a,b}, Bryce Taft^{a,b}, Charles Miksch^{a,b}, Talon Mills^a, John M. Dyer^a

^aU.S. Department of Agriculture, Agricultural Research Service, U.S. Arid-Land Agricultural Research Center, 21881 North Cardon Lane, Maricopa, AZ 85138, USA

^bMaricopa High School, College and Career Preparatory Academy, 45012 West Honeycutt Avenue, Maricopa, AZ 85139, USA

ARTICLE INFO

Article history:

Received 10 January 2018

Received in revised form 12 April 2018

Accepted 19 April 2018

Available online xxxx

Keywords:

Field-based high-throughput phenotyping
Platforms

Proximal sensing

Proximal imagery

ABSTRACT

An easy-to-customize, low-cost, low disturbance, motorized, and adjustable proximal sensing cart for field-based high-throughput phenotyping is described. General dimensions, motor specifications, and a remote operation application are given. The cart, named Professor, supports mounting multiple proximal sensors and cameras for characterizing plant traits grown under field conditions. Professor easily adapts to multiple sensor configurations supporting detection of multiple target traits and has two axes of adjustable clearance by design. Professor is useful as a field-based phenotyping platform and offers a framework for customized development and application.

Published by Elsevier Ltd. This is an open access article under the CC BY license (<http://creativecommons.org/licenses/by/4.0/>).

Specification

Hardware name	Professor
Subject area	Environmental, Planetary and Agricultural Sciences
Hardware type	Field measurements and sensors
Open Source License	U.S. Public Domain
Cost of Hardware	\$4000 (Without sensors or cameras)
Source File Repository [11]	http://dx.doi.org/10.15482/USDA.ADC/1431007

1. Introduction

Improving crop yield to meet the demands of a growing population is one of the biggest challenges faced by agriculture today [1]. The estimated increase of the world's population to 9 billion by 2050 will necessitate a >70% increase in agricultural production worldwide to meet growing demands in food, fiber, and bioenergy [2]. One of the biggest bottlenecks to crop improvement is the ability to rapidly phenotype large numbers of field grown plants at regular intervals throughout the crops growth cycle [3]. Current manual techniques are labor intensive and time consuming, and often introduce variation

* Corresponding author.

E-mail address: alison.thompson@ars.usda.gov (A.L. Thompson).

in the collected data [4]. To improve crop yields and quality, novel phenotyping approaches are needed to rapidly capture plant traits in the field.

Field-based high-throughput phenotyping (FB-HTP) is a novel approach to rapidly characterize (>1 m plot transect/second) plant traits using proximal and remote sensing or imaging. Current proximal sensing platforms include unmanned aerial systems (UAS), high-clearance tractors or other field implements, field scanners, and field carts [5]. Field carts for proximal sensing are typically low-cost, narrow-wheeled, lightweight platforms that have low soil disturbance, are easy to maneuver and transport, and can be designed to accommodate specific crop height and row spacing's, while deploying multiple sensors [6–8]. This enables users to deploy the cart and collect multiple plant traits across an extended duration and location range, as compared to UAS sensor payload and duration, and high-clearance tractors location range. Limitations of manually operated field carts include soil interface z-plane displacement anomalies (bumps), operator fatigue, and inconsistent collection speeds, all of which can affect data quality. Commercial field carts have been developed with drive-assisted technology to alleviate some of these limitations [7], but these are typically not fully customizable or openly available. Open source, low-cost cart options are needed by the scientific community to support research programs with limited budgets and/or with varied agronomic applications.

This paper presents Professor, an adaptable, low-cost, electric, motorized, remote-controlled, and adjustable field cart platform suitable for proximal sensing and imaging in a wide range of agricultural and environmental settings. This system utilizes readily available products for the frame, drive train, and remote control to alleviate the limitations of previous cart models. Professor is fully customizable to accommodate different crops, field designs, and proximal sensing arrays. The design presented in this paper was produced in full cooperation with local high school students, to educate and develop math and mechanical engineering awareness and skillsets, and to provide simple mechanical solutions that support solving complex field phenotyping problems.

2. Materials

All of the components needed for the assembly of Professor are listed in S. File 1. These standardized components are easy to obtain and relatively inexpensive, which enables replication or customization of Professor, based on program goals and available resources. How to build Professor is described in detail below.

3. Methods

The cart is comprised of a frame, wheel assembly, drive train, controller, battery, and the proximal sensing array(s). The sensing array(s) and data recording system (i.e. laptop or data logger) are mounted to the inner frame (Fig. 1)

Design Files Summary			
Design file name	File type	Open source license	Location of file
S. File 1	XLSX	U.S. Public Domain	http://dx.doi.org/10.15482/USDA.ADC/1431007
S. File 2	PDF	U.S. Public Domain	http://dx.doi.org/10.15482/USDA.ADC/1431007
S. File 3	PDF	U.S. Public Domain	http://dx.doi.org/10.15482/USDA.ADC/1431007
S. File 4	PDF	U.S. Public Domain	http://dx.doi.org/10.15482/USDA.ADC/1431007
S. File 5	PDF	U.S. Public Domain	http://dx.doi.org/10.15482/USDA.ADC/1431007
S. File 6	PDF	U.S. Public Domain	http://dx.doi.org/10.15482/USDA.ADC/1431007
S. File 7	XLSX	U.S. Public Domain	http://dx.doi.org/10.15482/USDA.ADC/1431007

Nomenclature key:

Height = h; Width = w; Length = l; Thickness = t; Inner diameter = id; Outer diameter = od.

3.1. Cart frame

3.1.1. Dimensions and structure

The cart is constructed primarily from 40 × 40 mm extruded aluminum T-Slot, framing members, and hardware (80/20 Inc., Columbia City, IN) (S. File 1). The cart consists of two frames, the outer frame and the inner frame, which are fully adjustable. The outer frame can increase/decrease in width to accommodate different row-spacing configurations and the inner frame can increase/decrease in height to accommodate different crop canopy architectures. The outer frame is approximately 200.0 × 207.2 × 190.0 cm (h × w × l), which supports the inner frame and is attached to the wheel assemblies. The inner frame is clamped inside the outer frame and is approximately 33.0 × 208.0 × 170.0 cm (h × w × l) (Fig. 2). The brackets that connect the inner frame to the outer frame, made from the same aluminum T-slot, are 16.0 × 25.0 × 4.0 cm (Fig. 2). The top and bottom of each bracket are attached to the inner frame by two flat aluminum plates, 16.0 × 10.16 × 0.64 cm. The plates hold the inner frame away from the bracket by 1.4 cm. A slider piece is bolted to the bracket and the vertical outer frame support bars move through the slider by loosening the wing nuts, allowing for vertical movement of

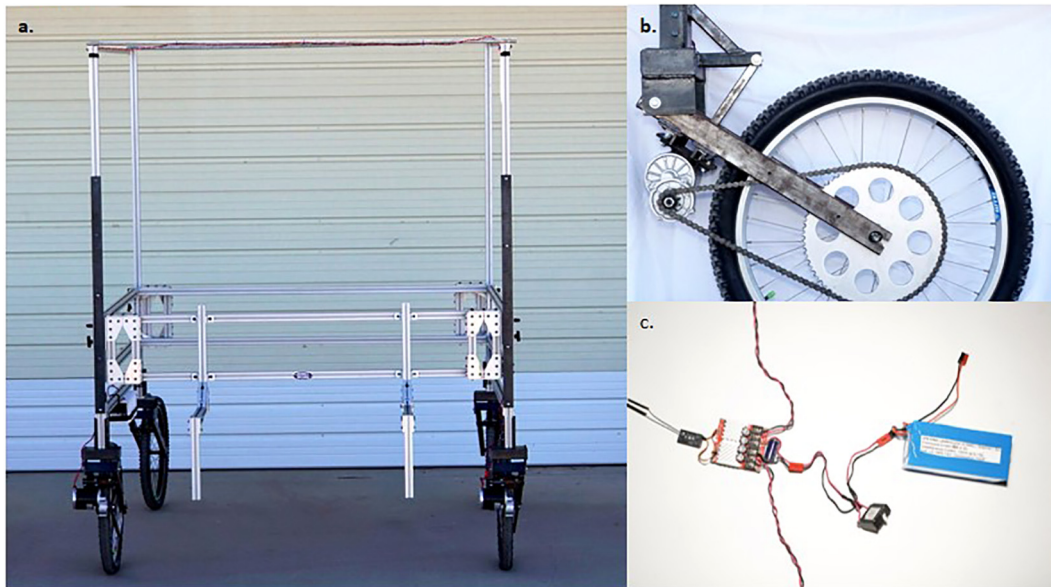


Fig. 1. Assembled frames (a), drives wheels (b), and electrical components (c) of Professor: A Motorized Field-Based Phenotyping Cart.

the inner frame. The width of the outer frame can be adjusted by loosening the bolts on the flat plates that connect the bracket to the inner frame. The outer frame is strengthened with $0.64 \times 5.08 \times 116.84$ cm ($t \times w \times l$) steel rectangle bars on the front to minimize flex when the inner frame is raised to 200.0 cm, the highest position for this configuration (Fig. 2). To help stabilize the outer frame and reduce twisting about the brackets, a $0.32 \times 2.54 \times 2.54 \times 190$ cm ($t \times w \times h \times l$) aluminum 90° bar is connected to the top of the vertical arms from front to back. Horizontal support is provided by a 1.59 cm diameter tube of galvanized steel, attached with a small piece of sheet metal wrapped around the tube and bolted to the top of the outer frame and clamping it in place (Fig. 2). This way, the bolts can be loosened and allow effective width adjustment.

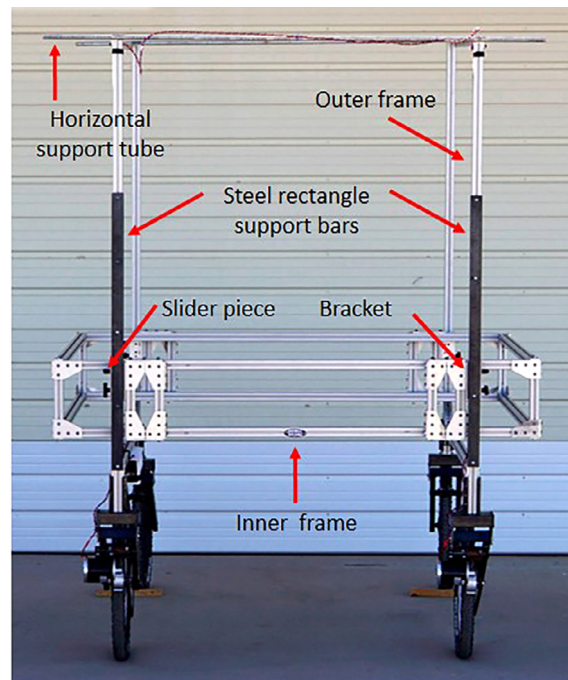


Fig. 2. The T-slot assembled inner and outer frames of Professor with key features identified by the red arrows. This configuration shows Professor set at 150 cm \times 152.4 cm ($h \times w$).

3.2. Wheel assembly

3.2.1. Swivel wheels

The wheels for the swivel wheel assembly are standard 66.04×4.45 cm (26×1.75 in) front mountain bicycle wheels with a 10 cm hub. The build is modeled after a bicycle front wheel fork assembly where the outer tube is fixed to the frame, and the inner tube is attached through headset bearings. This allows for use of a standard 2.86 cm Venzo threadless mountain bike sealed headset for the swivel wheel assembly bearings. The assembly is built by welding the header tube, $3.4 \times 0.64 \times 15.24$ cm ($id \times t \times l$), to the bracket that attaches to the outer frame. The bracket is made from three pieces of rectangular steel bar with two pieces, $0.64 \times 5.08 \times 15.24$ cm ($t \times w \times l$), welded perpendicular to the third, $0.64 \times 7.62 \times 15.24$ cm ($t \times w \times l$). The two smaller pieces are welded with a spacing of 40 mm to fit around the T-slot. The headset is seated inside the header tube. The portion of the swivel wheel assembly that turns relative to the frame is built with a $2.86 \times 0.64 \times 27.94$ cm ($od \times t \times l$) steer tube, welded inside a 2.86 cm hole drilled in the center of a larger rectangular $0.62 \times 10.16 \times 5.08 \times 17.15$ cm ($t \times w \times h \times l$) tube ($t \times w \times h \times l$). The steer tube is connected to the header tube via the bearing headset (Fig. 3, S. File 2). Additional $0.64 \times 7.62 \times 10.16$ cm ($t \times w \times l$) brackets are welded to the base of the rectangular tube 16.51 cm apart and represent the attachment points to the wheel support arms using a bushing. The support arms are built from $0.48 \times 2.54 \times 5.08 \times 55.88$ cm ($t \times w \times h \times l$) rectangular tubes that are welded into a spacing of 10.48 cm, using two $0.64 \times 5.08 \times 16.51$ cm ($t \times w \times l$) steel rectangle bars (S. File 3). One bar is attached to the end of the arms nearest the mount connection and the other on the bottom side 12.7 cm from the end. The wheel is attached after drilling a 1 cm diameter hole, 2.54 cm from the end and sides of the arm. A notch is cut out of the end of the arm to allow the wheel to slide into place where the hole is drilled. The outer of the two holes in the rectangular tubing is drilled out even larger, 2.86 cm diameter, to allow socket wrench access to tighten the wheel nut. A $0.32 \times 2.54 \times 2.54 \times 21.59$ cm ($t \times w \times h \times l$) square tube fixes the angle of the support arm in place. The square tube is attached through two additional brackets, one made with two $0.64 \times 2.54 \times 2.54 \times 5.08$ cm ($t \times w \times h \times l$) 90° angle aluminum pieces bolted to the support arms and a $0.48 \times 5.08 \times 2.54 \times 12.70$ cm ($t \times w \times h \times l$) piece of u-channel steel welded to the side of the large rectangular support tube. An additional piece of angle iron, $0.32 \times 3.81 \times 3.81 \times 16.51$ cm ($t \times w \times h \times l$), is welded below the u-channel for support (Fig. 3, S. File 2).

3.2.2. Drive wheels

The drive wheels are standard 66.04×4.45 (26×1.75 in) front mountain bicycle wheels with 6-hole disc brake compatible 10 cm hubs. These hubs contain a quick release axle that does not leave sufficient room for attaching the wheel support arms. The axels were replaced with $10 \times 1 \times 174$ mm solid axels and 10×1 axel nuts with washers. The main supports for the drive wheels are similar to the swivel wheel supports in construction, but with a few critical differences. First, the main bracket that is attached to the primary frame is welded directly to the $0.62 \times 10.16 \times 5.08 \times 17.15$ cm ($t \times w \times h \times l$) rectangular tube. Second, an additional support, $0.48 \times 2.54 \times 5.08 \times 15.24$ cm ($t \times w \times h \times l$), is welded 45° to the outer frame bracket at the top of the u-channel instead of the angle iron and provides increased support for the heavier front end. An additional $0.64 \times 5.08 \times 16.51$ cm ($t \times w \times l$) steel rectangle bar is added 7.62 cm from the top of the arm for the motor mount. Third, two additional $0.64 \times 5.08 \times 10.16$ cm ($t \times w \times l$) steel rectangular bars are welded to the sides of the main rectangular tube to close off the ends and increase mechanical support (Fig. 4, S. File 4).

3.3. Drive train

3.3.1. Motor

The basic design of the drive train uses a gear reduction electric motor with a chain drive. The chain connects to a custom built sprocket on the corresponding drive wheel via the disc brake hub. Each drive wheel has its own drive assembly that is



Fig. 3. The rear mounted swivel wheel assembly with key features identified by the red arrows.

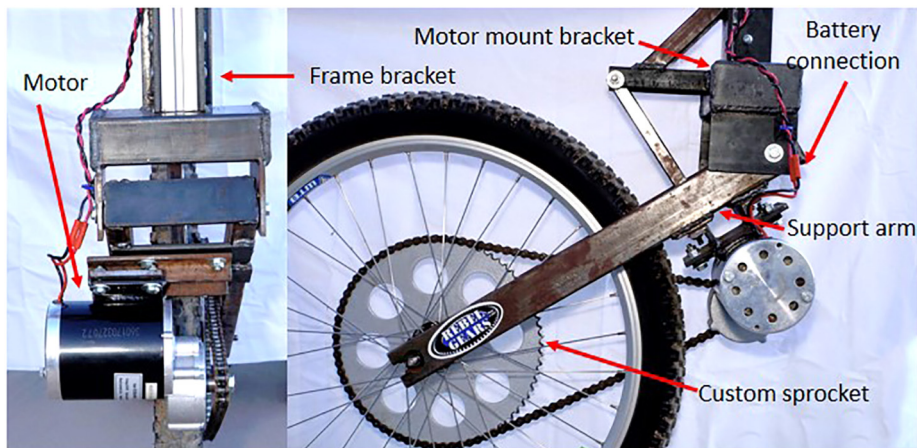


Fig. 4. The front mounted drive wheel assembly and motor with key features identified by the red arrows.

independently controlled through the main controller for a minimal turning radius. The motors are mounted to the bottom of the drive wheel arms (Fig. 4, S. File 5). The motor mount brackets are made by welding two $0.64 \times 2.54 \times 2.54 \times 15.24$ cm ($t \times w \times h \times l$) steel angle bars perpendicular to a $0.64 \times 7.62 \times 13.97$ cm ($t \times w \times l$) steel rectangle bar. The angle iron pieces are bolted to the brackets on the bottom of the support arms, and the motor is bolted to the flat plate. The drilled holes in the flat plate that the motor is mounted to are slotted, so that the motor can slide up or down to tension the chain.

3.3.2. Sprocket and gearing

The custom built sprocket by Rebel Gears, has 72 teeth for a #40 chain and has 6 bolt holes (.55 cm diameter) spaced evenly around (4.4 cm diameter) the 3.4 cm diameter center bolt hole (S. File 6). The hub mounting holes are specified for standard mountain bike 6-bolt disc brake dimensions. The sprockets are bolted to the wheel hub with a washer spacer on the main axle to ensure there is room for the chain and bolts to turn without hitting the support arm (Fig. 4).

3.4. Controller and battery

3.4.1. Control board

The RoboClaw 2x60AHV 60 V DC control board is versatile, easy to use, and works with high voltage motors. An easy to use computer program, IonStudio (Ion Motion Control, Temecula, CA) www.ionmc.com, allows for quick setup of the control board through a USB port. The configuration used for the control board settings are remote control (R/C) mode with a pulse-width modulation (PWM) mode of locked antiphase. The R/C settings are: 1) mixing, 2) exponential, and 3) micro or motor controller unit (MCU). Mixing enables motor control so that one channel controls forward and backward, and the other controls turning (Fig. 5). Exponential reduces sensitivity to inputs when starting from a stop, making control easier when at low speeds. MCU disables the auto calibrate function. A dead band range, or stop position of 6.5% is used so that Professor will not creep in motion with the controller stick centered (in the off position). Maximum and minimum battery voltage settings were selected to match the safe values for the selected battery. The values set for the motors are to limit the motor current to 24.9 amps, and a motor acceleration of 50,000 and deceleration of 10,000. These values are out of a maximum of 655,360. The values were chosen via extensive testing to ensure the cart would not tip when the controller was released from full speed. The need for these acceleration settings is due to the regenerative braking capability of the controller and are used to prevent Professor from tipping forward when stopping too quickly.

3.4.2. Transmitter and receiver

The transmitter and receiver is a FrSky Taranis X9D PLUS transmitter with an X8R receiver. Only two channels are needed. The transmitter is setup so that the left control stick (S1) moves Professor forward or back while the right stick (S2) controls turning (Fig. 6). The FrSky Taranis has many options for configuration and programmability including the ability to trim either of the two channels. The channel trim ensures the cart will not move when the controls are not being used and keep the cart in a straight line when driving. For Professor, a switch is programmed to activate a constant throttle value while still allowing the user to steer without slowing down. This allows for a constant speed to ensure steady data capture.

3.4.3. Battery

The battery used to power Professor is an ElectroRide 37 V, 13 Ah LiNMC battery (Fig. 7a). A custom made wooden box $12.5 \times 12.5 \times 38.0$ cm ($h \times w \times l$) houses the battery and is bolted to the bottom support arm of the outer frame (Fig. 7b).

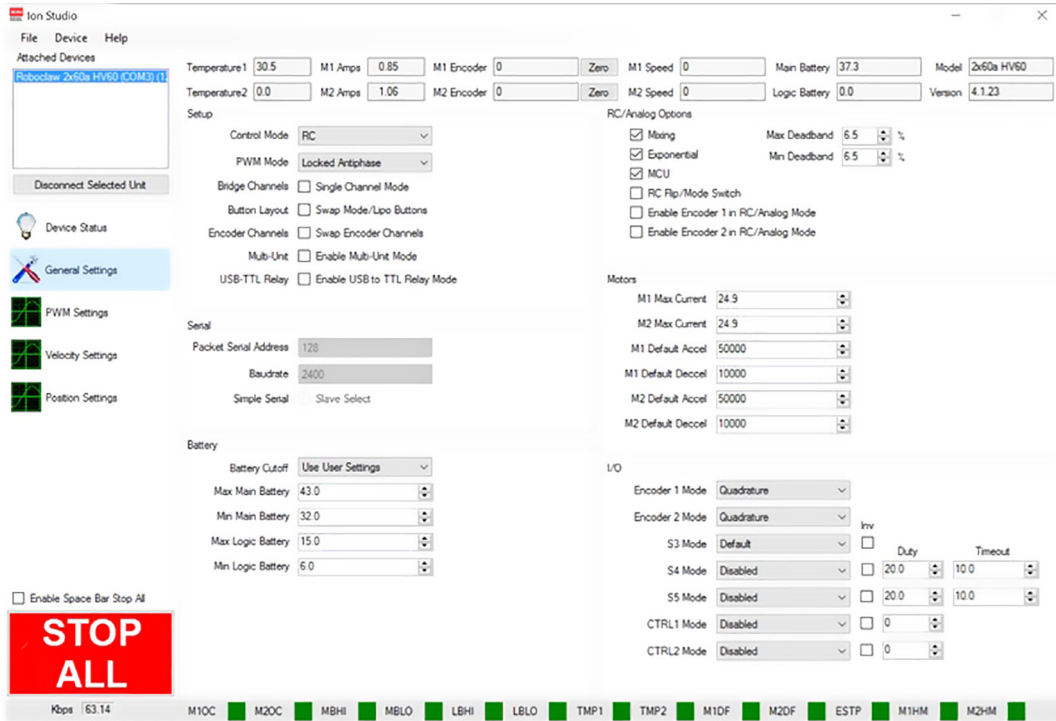


Fig. 5. Professor program settings for FrSky Taranis remote control using Ion Studio software.



Fig. 6. FrSky Taranis Plus transmitter and receiver for remote control of Professor.

3.4.4. Wire connections

Channel 1 and 2 on the receiver are directly connected to S1 (left stick) and S2 (right stick) on the motor controller respectively. The 5 V power for the receiver comes directly from the motor controller board. Both motors are wired directly into the motor controller with the left motor red wire connected to terminal M1A and the black into M1B. The right motor is reversed with the black wire in M2A and the red in M2B. The battery is wired directly into the controller with a 50 amp DC breaker and a 2200 μF capacitor across the battery wires at the connection point of the control board. A diode is placed in reverse across the breaker switch so that if the switch is disconnected while moving there would still be a path for the current generated by the motors back to the battery (Fig. 7c and d).

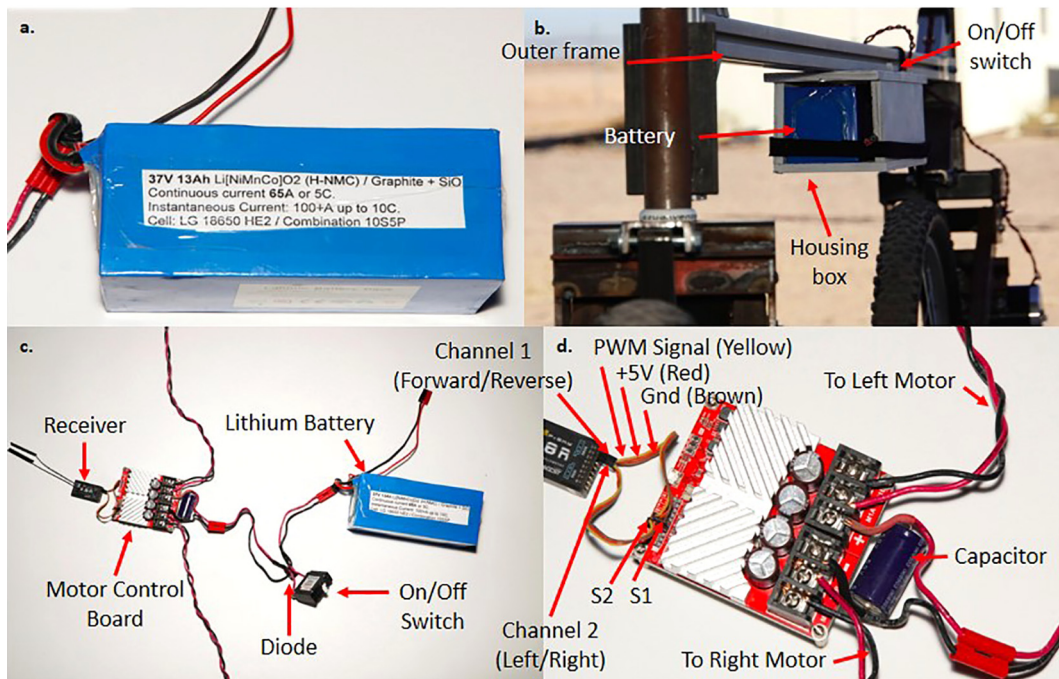


Fig. 7. Lithium battery (a), frame mounted housing box (b), and connections between battery and motors to the receiver (c and d).

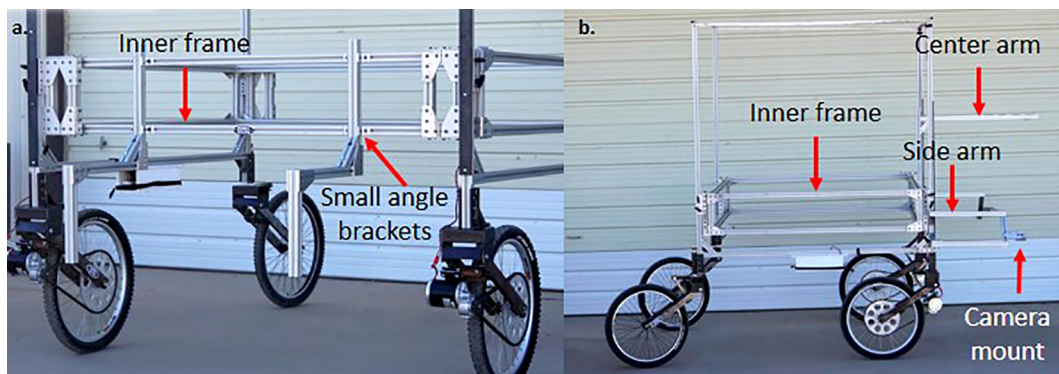


Fig. 8. Proximal sensor array (a) and image sensor array (b).

3.5. Sensor arrays

3.5.1. Mounting arms for proximal sensor array

Professor is designed to transport a proximal sensor array similar to those described by Bai et al. [6], White and Conley [8], Andrade-Sanchez et al. [9], and Barker et al. [10]. The mounting arms are each built from three pieces of 40 mm T-slot. A 50 cm bar connects vertically to the inner frame through 4 small angle brackets. Another 50 cm horizontal bar connects to the vertical bar through a 16 cm 45° brace and 4-hole side brackets. Finally, a 40 cm drop down bar is attached using 4-hole brackets connected to the end of the horizontal bar (Fig. 8a).

3.5.2. Mounting arms for image sensor array

There are two types of mounting arms used for the image sensor array. The center arm is built from two 1 m bars of 40 mm T-slot and is connected directly to the inner frame through four small brackets. A 16 cm 45° brace is used to connect the horizontal bar to the top of the vertical one. Second, two side-mounted arms are constructed from two 60 cm bars protruding forward. The lower piece is offset outwards by a separate T-slot bar 25 cm long. At the front, the two pieces are fixed together by a 32 cm long 45° brace that provides an angled camera mount space. The 25 cm and top 60 cm pieces are mated directly to the side of the outer frame vertical bars (Fig. 8b).

Table 1

The drive time for each 12.1 m plot for three replicates (Pass) as recorded by a Hemisphere GPS receiver and Campbell Scientific data logger. The average time per plot is calculated below. The difference in time for each plot from the average is listed in the Difference column. Time is listed as minute:second.millisecond.

Plot	Pass	Time	Difference	Pass	Time	Difference	Pass	Time	Difference
717	1	00:38.0	00:00.2	2	00:38.8	00:00.5	3	00:38.0	00:00.3
718	1	00:38.6	00:00.4	2	00:39.6	00:01.3	3	00:38.4	00:00.7
719	1	00:39.2	00:01.0	2	00:40.0	00:01.7	3	00:38.2	00:00.5
720	1	00:38.8	00:00.6	2	00:39.0	00:00.7	3	00:38.2	00:00.5
721	1	00:38.6	00:00.4	2	00:39.0	00:00.7	3	00:38.0	00:00.3
722	1	00:38.6	00:00.4	2	00:38.4	00:00.1	3	00:38.0	00:00.3
723	1	00:34.6	00:04.4	2	00:35.6	00:02.7	3	00:35.0	00:02.7
724	1*	01:06.8	00:28.6	2	00:38.8	00:00.5	3	00:37.8	00:00.1
817	1*	01:07.0	00:28.8	2	01:00.8	00:22.5	3	n/a	n/a
818	1	00:36.0	00:02.2	2	00:35.8	00:02.5	3	n/a	n/a
819	1	00:38.8	00:00.6	2	00:38.6	00:00.3	3	n/a	n/a
820	1	00:39.0	00:00.8	2	00:38.8	00:00.5	3	n/a	n/a
821	1	00:39.0	00:00.8	2	00:38.6	00:00.3	3	n/a	n/a
822	1	00:38.6	00:00.4	2	00:38.0	00:00.3	3	n/a	n/a
823	1	00:38.4	00:00.2	2	00:37.6	00:00.7	3	n/a	n/a
824	1	00:39.0	00:00.8	2	00:37.6	00:00.7	3	n/a	n/a
Average		00:38.2	00:00.9		00:38.3	00:00.9		00:37.7	00:00.7

* These plots are at the beginning/end of a pass and lead up onto the road. The duration of time for these plots is longer due to traffic and were not included in the average calculation.

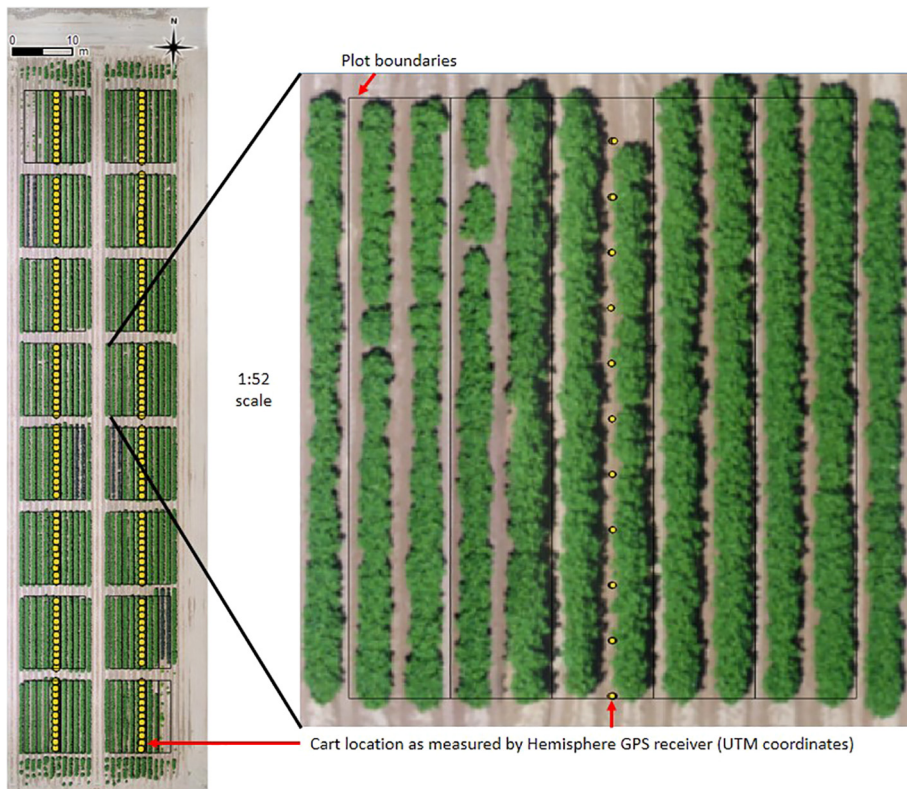


Fig. 9. Cart location measured by a Hemisphere GPS receiver (UTM coordinates) and recorded on a Campbell Scientific data logger while driving through the field. Cart coordinates are visualized in Quantum GIS over a field raster layer.

4. Performance and evaluation

Professor is adjustable and versatile, with linear clamping sliders making vertical adjustment relatively easy, and lateral wheel track adjustment after loosening bracket bolts. The T-slot constructed frame with motor and swivel wheel assembly is approximately 180 kg (397 lbs.) in total. Mechanical stress on the vertical members of the outer frame was detected,

especially when configured in the highest vertical clearance positions, but was alleviated with the addition of the rectangular steel bars described above. Professor can accommodate a sensor payload of at least 34 kg (75 lbs), as tested that can be mounted anywhere on the inner frame without diminishing field performance. However with loaded sensor arms in front, the center of mass is shifted far enough forward to make tipping a safety concern, particularly if stopping or beginning to reverse rapidly ($0\text{--}2.31\text{ m s}^{-1}$ in 2 s). During field operation there was some vibration and bounce at the end of the attached proximal sensor arms ($\sim 1\text{ cm}$ max full amplitude at $10\text{--}20\text{ Hz}$). The relatively tall tire height helped to reduce mechanical displacement artifacts common in agricultural fields (Video 1).

Professor's torque and power drive capabilities were sufficient for a proximal sensing phenotyping field application. The custom sprocket, along with the 10 tooth drive gear on the motor, delivers a gear ratio of 7.2 that, when combined with the maximum 480 RPM of the motor and 66 cm tire diameter, yielded a maximum no load speed of 2.31 m s^{-1} (5.2 mph). In the field, Professor was easily able to maintain a constant speed of 0.32 m s^{-1} (0.72 mph), and could be quickly corrected if a small obstacle offset the course. The average time to cover each 12.1 m plot was 38.1 s and an average difference from the mean at 8 ms (Table 1; S. File 7). The swivel wheel setup, combined with two independent drive motors, allowed for very precise control and placement of Professor (Fig. 9). The swivel wheel setup also allowed for excellent maneuverability. It was possible to exit a row in the field and turn 180° while keeping one drive wheel in the same place and then proceed down the next row (Video 2). Professor had little to no issues climbing over small field obstacles such as soil clods or the irrigation berms or traversing loose soil or sand (S. Videos 1–4) (<http://dx.doi.org/10.15482/USDA.ADC/1431007>).

Professor was also tested in wheat and early season maize fields. The row-spacing for the wheat and maize crop was planted on 30-in centers, requiring the outer frame to be adjusted to a narrower width. Cart adjustment takes three people approximately 15 min (S. Fig. 1). As the maize crop was not fully mature the cart frame had no problems clearing the plants. Should late season measurements of maize be required, modifications to the overall frame height would likely need to be made. Camera and sensor placement for data capture were not tested in the wheat or maize field. Future work is needed to determine if the sensor arrays would need adjustment to accommodate these other crops.

The lithium battery charge voltage range spans $32\text{--}42\text{ V}$ in a 10S5P configuration, and supplied a total 481 Watt-hours of energy. Running full speed (2.31 m s^{-1}), the power consumption of Professor is over 1200 Watts, but for typical field



Fig. 10. Example images captured by Professor from each camera mounted to the image sensor array in nadir view (a), left oblique view (b), and right oblique view (c). A three-dimensional point cloud (d) and orthomosaic (e) developed from the example images using Agisoft Photoscan Professional software.

operation speed (0.32 m s^{-1}) only 75–150 Watts was consumed. This resulted in a functional duration of up to 5 h, primarily dependent on speed, payload, and field conditions.

5. Example application

Professor was designed to accommodate multiple proximal sensor arrays, however, in this iteration the image sensor array has been utilized. The Professor's square frame provides excellent opportunities to mount cameras in field of view optimized positions relative to the field grown crops, and accommodate external lighting or shading equipment. By design, Professor's internal box volume provides ample space to implement full illumination control.

In this example, the image sensor array (described above), under natural lighting, was tested with simple Canon PowerShot SX600 HS with 16.8 MP (Canon Inc. Melville, NY) cameras, set for continuous capture. Sample images from this deployment are provided in Fig. 10a–c. These images were used to generate a 3-dimensional (3D) point cloud (Fig. 10d) and orthomosaic (Fig. 10e) of the cotton crop using Agisoft Photoscan Professional software v. 1.3.2 (St. Petersburg, Russia).

6. Conclusion

Professor is a low-cost, flexible, motorized field phenotyping cart that can be used for characterizing plant traits under field conditions. The cart was specifically designed to be low-cost and open-source to enable field-based high-throughput phenotyping for users with limited budgets and other resources. Professor has a small turning radius and fine motor control in both speed and direction of travel, allowing enhanced maneuverability and more consistent data collections. Additional improvements over traditional carts include re-designing the frames with a lighter, more rigid material to minimize flex and strain and support increased adjustment. Professor also provides opportunities for student involvement to design and develop material features that can be applied to real world agricultural challenges.

7. Funding

This research was supported by the United States Department of Agriculture–Agricultural Research Service 2020-21410-006-00D (A.L.T., J.M.D.) and a Cotton Incorporated Research Grant 13-738 (A.L.T.). Mention of trade names or commercial products in this publication is solely for the purpose of providing specific information, and does not imply recommendation or endorsement by the USDA. The USDA is an equal opportunity employer.

Acknowledgements

We would like to thank Maricopa High School for enabling this partnership and support and all students who applied to be part of this project. We thank Aaron Shwarts for contributions of ideas and Paige Francis for help with images.

Appendix A. Supplementary data

Supplementary data associated with this article can be found, in the online version, at <https://doi.org/10.1016/j.ohx.2018.e00025>.

References

- [1] R.T. Furbank, M. Tester, Phenomics – technologies to relieve the phenotyping bottleneck, *Trends Plant Sci.* 16 (12) (2011) 635–644.
- [2] M. Tester, P. Langridge, Breeding technologies to increase crop production in a changing world, *Science* 327 (2010) 818–822.
- [3] Y. Ge, G. Bai, V. Stoerger, J.C. Schnable, Temporal dynamics of maize plant growth, water use, and leaf water content using automated high throughput RGB and hyperspectral imaging, *Comput. Electr. Agri.* 127 (2016) 625–632.
- [4] J.M. Montes, A.E. Melchinger, J.C. Reif, Novel throughput phenotyping platforms in plant genetic studies, *Trends Plant Sci.* 12 (10) (2007) 433–436.
- [5] J.W. White, P. Andrade-Sanchez, M.A. Gore, K.F. Bronson, T.A. Coffelt, et al, Field-based phenomics for plant genetics research, *Field Crops Res.* 133 (2012) 101–112.
- [6] G. Bai, Y. Ge, W. Hussain, P.S. Baenziger, G. Graef, A multi-sensor system for high throughput field phenotyping in soybean and wheat breeding, *Comput. Electron. Agric.* 128 (2016) 181–192.
- [7] G.J. Rebetzke, J.A. Jimenez-Berni, W.D. Bovill, D.M. Deery, R.A. James, High-throughput phenotyping technologies allow accurate selection of stay-green, *J. Exp. Botany* 67 (17) (2016) 4919–4924.
- [8] J.W. White, M.M. Conley, A flexible, low-cost cart for proximal sensing, *Crop Sci.* 53 (2013) 1646–1649.
- [9] P. Andrade-Sanchez, M.A. Gore, J.Y. Heun, K.R. Thorp, A.E. Carmo-Silva, A. French, M.E. Salvucci, J.W. White, Development and evaluation of a field-based high-throughput phenotyping platform, *Functional Plant Bio.* 41 (2014) 68–79.
- [10] J. Barker, N. Zhang, J. Sharon, R. Steeves, X. Wang, Y. Wei, J. Poland, Development of a field-based high-throughput mobile phenotyping platform, *Comput. Electr. Ag.* 122 (2016) 74–85.
- [11] A. Thompson, Professor: A Motorized Field-Based Phenotyping Cart, *Ag Data Commons*, <http://dx.doi.org/10.15482/USDA.ADC/1431007>.